Water Harvesting Research Vol. 5, No. 2, Autumn & Winter 2022, Original Paper p. 177-190

University of Birjand

10.22077/JWHR.2023.6184.1079

Performance Assessment of Numerical Solution in Simulating Groundwater Recharge

Ahmad Jafarzadeh[a*], Abbas Khashei-Siuki[a], Abolfazl Akbarpour[b], Ali Nasirian[b]

[a]Department of Water Engineering, University of Birjand, Birjand, Iran.
[b]Department of Civil Engineering, University of Birjand, Birjand, Iran.

[*]Corresponding Author, E-mail address: mnt.jafarzadeh@gmail.com, http://orcid.org/0000-0003-4761-7940
Received: 5 March 2023/ **Revised**: 09 April 2023/ **Accepted**: 17 April 2023

Abstract

Aquifer regeneration is one of the essential primary solutions to better the crisis of these resources. Optimum locating of injection and considering the influencing factors of the aquifer's features are the most critical issues that have always been challenging for researchers. Hence, this study addressed the efficiency of two developed numerical methods in simulating artificial recharge. For this purpose, three scenarios were defined to evaluate the performance of numerical methods (comparison of analytical and numerical solutions), simulating the rise of the groundwater level, and analyzing the sensitivity of the hydrodynamic features of the aquifer. The concept of two numerical methods (i.e., Finite Difference 'FD' and Finite Element' FE') was performed as open-source coded in MATrix LABoratory (MATLAB), and their efficiency was examined. Results indicated that the simulated groundwater drawdown due to extraction wells is compatible with the analytical solutions regarding RMSE and NSE. Also, the performance evaluation results showed that the accuracy of the FE method is better than the FD. The experiment's results of artificial recharge into the aquifer through the injection well also showed that the groundwater level rise in the FE method is faster than in the finite difference method. Also, after 1500 days of recharge, the height of the groundwater level is up to about 90 cm.

Key words: Anisotropy, Heterogeneity, specific yield, Transmissivity, Weighted Residual Methods.

1. Introduction

Human activities have a significant and far-reaching impact on the environment, manifesting through factors such as climate change, rapid urbanization, overpopulation, pollution, and deforestation. Among these, the direct contact of human life with water resources results in severe consequences, such as pollution and depletion. Thus, effective conservation practices and sustainable land planning are essential for ensuring the responsible management of these vital resources. Furthermore, given that water resources are fundamental to development planning, regions endowed with substantial water resources are likely to experience rapid and stable growth (Mohammadi et al., 2020). In summary, safeguarding water resources is critical for promoting sustainable development and mitigating the adverse effects of human activities on the environment.

Literature indicated that groundwater sources are 1.7 percent of the whole water of Earth and one-third of freshwater is allocated to groundwater in the world (Hora et al., 2019). Also, the spatial distribution of groundwater is completely different in continents and countries. In some regions, these sources are used accompanied by surface sources to compensate for demands. Further, in some areas with weak potential in surface water, groundwater sources play a key role to meet all

needs (Hamidian et al., 2019). Hence, the status of the groundwater resources must be considered in future planning, and the development vision should be designed according to their quantitative and qualitative potential. So, the groundwater modeling can be a robust tool to draw a future image for implementing plans, because the requirement for efficient planning is identification, knowledge, and detailed information about the conditions (Liu et al., 2019).

Groundwater modeling can be spatially divided into three major types: first lumped modeling in which the simulation of key features is accomplished across the aquifer (i.e., the problem domain is the whole aquifer). This process seeks to give a general estimate of the quantitative and qualitative status of the aquifer and it seems the best option in limited-data cases (Jafarzadeh et al., 2021). Although the less computational burden and fewer numbers of parameters for optimization lead the lumped modeling attractive for groundwater simulation (e.g., Mackay et al. 2014), the existing uncertainty of these models is significant due to simplifying assumptions resulting in the unreliable prediction of groundwater process.

Numerical modeling of groundwater level is crucial for managing and sustaining groundwater resources. It provides valuable insights into the behavior of aquifers and helps to predict changes in groundwater levels due to various factors such as pumping, recharge, and climate change. Additionally, numerical modeling can aid in identifying optimal locations for well placement, designing effective groundwater management strategies, and evaluating the impact of human activities on groundwater resources. This modeling requires a deep knowledge of aquifer features, including anisotropy and heterogeneity, of the system (Shepley et al., 2012), and imposes more time and cost on the modeler. However, the final prediction is the more reliable, and the real world can be resolved through them. Finite difference (FD) and finite element (FE) techniques are among the more promoting numerical methods applied frequently for groundwater context.

The simplicity and quick run of FD, the oldest and simplest numerical method, lead the Computational Fluid Dynamic 'CFD' pioneers to develop the MODular groundwater FLOW (MODFLOW), most widely used model in groundwater media, through FD (McDonald and Harbaugh, 1984). Currently, FD is utilized for different targets including groundwater protection (Pacheco et al., 2018), estimating aquifer depletion (Fletcher et al. 2019), hydrodynamic factors determination (Xu et al. 2017), uncertainty analysis (Hamraz et al., 2015), surface recharge along with evaporation, climate change impacts (Maquin et al., 2017). However, the application of FD in real-world cases whose geometry is irregular has some problem resulting uncertainty. FE methods, developed by some pioneers (e.g., Zienkiewicz et al., 1966; Javandel and Witherspoon, 1968) in groundwater context, overcome this issue and present approximated numerical solution for both regular and irregular domains.

In addition, arid regions worldwide are grappling with excessive groundwater extraction, resulting from an imbalance between recharge and extraction volume. To address this issue, it is crucial to reevaluate the management and maintenance of these resources.

One of the most important conserving practices is the artificial recharge of the aquifer through non-conventional water sources such as treated sewage, urban runoff, etc. (Hussain et al., 2019). Artificial recharge is accomplished for different goals including quality improvement, raising groundwater levels, preventing the salt water intrusion, and controlling land subsidence (Norouzi and Shahmohammadi-Kalalagh, 2019). There is a widespread literature about artificial recharge into groundwater (e.g., Zaresefat et al., 2022; Sardo and Jalalkamali, 2022; Sadeghi and Hosseini, 2023). For example, Norouzi and Shahmohammadi-Kalalagh, (2019) focused to identify the potential zones of groundwater artificial recharge in Shabestar region, northwest of Iran. They employed the random forest (RF) model, a learning method based on ensemble decision trees, was proposed for locating in which slope and slope aspect, soil texture, erosion, land use, groundwater quality, permeability, and geological lithology were considered as influencing factors. In other study, Sadeghi and Hosseini (2023) delineated the potential groundwater recharge zones in

areas prone to saltwater intrusion hazard in central region of Iran. They developed an overlay-index methodology to delineate favorable GAR zones by a linear combination of 11 influential thematic layers in GIS. However, comparison of efficiency of different numerical methods in simulating groundwater recharge at same time has been yet received the less attention. Further, considering the complicated context of groundwater media such as heterogeneity and anisotropy were generally ignored in above mentioned studies.

Based on the available literature, there have been limited studies conducted on groundwater recharge using various numerical methods. Additionally, previous investigations have not fully accounted for the heterogeneous and anisotropic properties of the aquifer, indicating a significant research gap in this area. To address this gap, our study aims to evaluate the effectiveness of two distinct numerical models - Finite Difference (FD) and Finite Element (FE) - in simulating groundwater recharge in a synthetic aquifer. By considering the complex properties of the groundwater media, we seek to provide a more accurate representation of the processes involved in groundwater recharge. Furthermore, the study aims to identify and analyze any structural uncertainty associated with the use of these numerical methods, providing insights that can inform future research in this field.

2. Material and Methods

2.1. Groundwater Flow-Governing Equations

The governing equation of groundwater flow for two dimensional, isotropic and homogenous aquifers is given by (Arnold et al., 1993):

$$K.h\frac{\partial^2 h}{\partial x^2}+K.h\frac{\partial^2 h}{\partial y^2}+Q(i,j)=S_y\frac{\partial h}{\partial t},\quad \left(Q(i,j)=q+\sum_{i=1}^{n}Q_i\delta(x_o-x_i,y_o-y_i)\right) \tag{1}$$

Considering following boundary and initial conditions:

$$\frac{\partial h}{\partial \Gamma t}=\frac{q_t}{K}\Rightarrow on\quad \Gamma=\Gamma t$$
$$h(x,y,t)=\bar{h}\Rightarrow on\quad \Gamma=\Gamma u \tag{2}$$
$$h(x,y,o)=h_0\Rightarrow on\quad \Omega$$

where h, Sy, K, t are potential groundwater level (m), specific yield, hydraulic conductivity in horizontal and vertical direction (m/day), time (day). While Q, q and δ are source or sink function (m3/day), distributed rate of recharge or evapotranspiration over aquifer domain (m/day) and Dirac Delta function respectively. Also, $qt,\bar{h},h_0$ are known inflow rate (m^2/day), constant groundwater level (m), and initial head (m). Furthermore, $\Gamma,\Gamma t,\Gamma u$ are global, essential (Dirichlet) and natural (Neuman) boundary conditions respectively, while Ω indicates aquifer domain.

The approximated solutions of above equation were numerically are available through two both methods whose formulations are provided in proceed.

2.2. Finite Difference (FD)

Taking the Taylor series approximation, the space derivatives of h in horizontal and vertical directions can be calculated for each point. The change of variable $v=h^2$ is imposed into to Eq. 1, to simplify computations for unconfined aquifer. Finally, using the forward difference approximation for time derivatives, the fully implicit of FD is given by:

$$v_{i,j}^{t+1}=\left(\frac{1}{\omega+1}\right)*\left(\begin{array}{l}\left(\frac{v_{i+1,j}^{t+1}+v_{i-1,j}^{t+1}+v_{i,j+1}^{t+1}+v_{i,j-1}^{t+1}}{4}\right)\\ +\left[\omega*v_{i,j}^{t}\right]+\left[\frac{Q_{i,j}}{4*K}\right]\end{array}\right) \tag{3}$$

where,

$$\omega=\frac{S_y*a^2}{4*K*dt.\sqrt{v_{i,j}^{t}}},\ a=\Delta x=\Delta y$$

In the last, the groundwater level is obtained by using $h=\sqrt{v}$.

2.3. Finite Element (FE)

This study used triangular element due to simplify in implementation and successful performance. Therefore, the global domain of aquifer was divided to many elements and

calculation was performed on each element. The First step in FE is trial solution definition:

$$\hat{h}(x,y) = \sum_{L=1}^{n} h_L N_L(x,y) \quad (4)$$

where $\hat{h}(x,y)$ is trial solution (m), h_L: is groundwater level for Lth node, n: total number of nodes in aquifer domain and $N_L(x,y)$: is shape function. By substituting Eq.4 into Eq. 1, and using fundamental assumption of Weighted Residual Methods (WRMs):

$$\int_{\Omega} \left(\begin{array}{l} Kh\left(\frac{\partial^2 \hat{h}}{\partial x^2} + \frac{\partial^2 \hat{h}}{\partial y^2}\right) \\ +Q(i,j) - S_y \frac{\partial \hat{h}}{\partial t} \end{array} \right) W_L . d\Omega = 0 \quad (5)$$

where W_L is weight function that in FE method is similar to shape function based on Galerkin approach. The formulation of shape function for a specific triangular element consisted of i, j, and k vertices, is given by:

$$\begin{aligned} N_i &= \frac{1}{2A}\left[(x_k y_j - x_j y_k) + (y_k - y_j)x + (x_j - x_k)y\right] \\ N_j &= \frac{1}{2A}\left[(x_k y_j - x_j y_k) + (y_k - y_j)x + (x_j - x_k)y\right] \\ N_k &= \frac{1}{2A}\left[(x_k y_j - x_j y_k) + (y_k - y_j)x + (x_j - x_k)y\right] \end{aligned} \quad (6)$$

where A: is the area of triangular element. Using the integration by part in Eq.5, the second spatial derivatives of $\hat{h}$ is converted to first spatial derivatives of $\hat{h}$ and N_L. Regarding Eq.6, these spatial derivatives are calculated and final matrix form of FE is obtained. Considering forward approximation, the fully implicit scheme is given by:

$$\left([G] + \frac{[P]}{\Delta t}\right) . \left\{h^{t+1}\right\} = \left(\frac{[P]}{\Delta t}\right) . \left\{h^{t}\right\} + \{B_L\} + \{F_L\} \quad (7)$$

where [G] is the conductance matrix, [P] is the mass matrix, {F} is the boundary flux and, {B} is the load vector. The schematic layout of the FE method is displayed in Figure 1. For more information about FD and FE formulation see related studies (Jafarzadeh et al., 2021; Jafarzadeh et al., 2022)

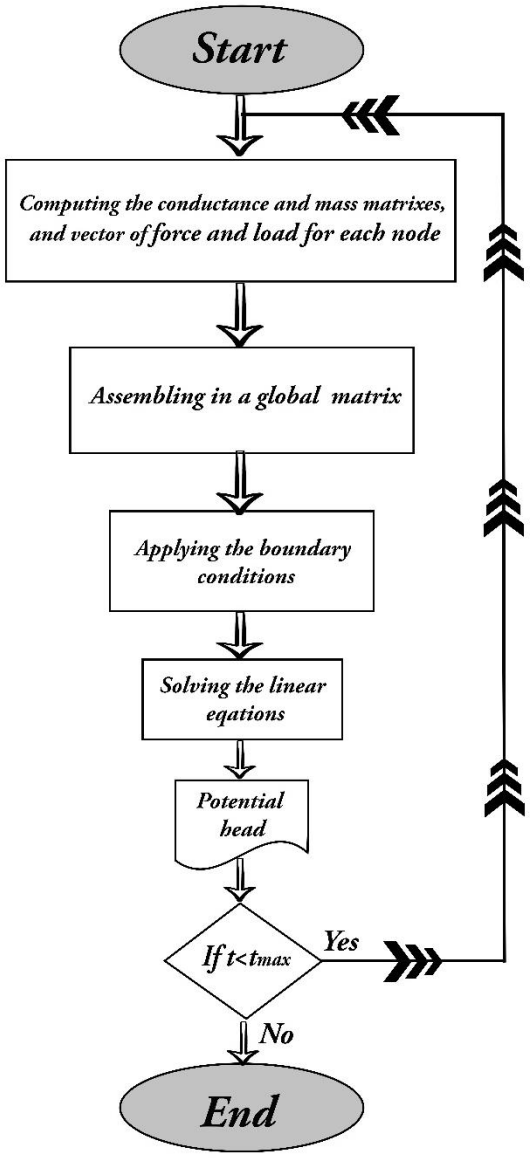

Fig. 1. Flow chart showing applied steps of FE models

The all applied steps of above mentioned were implemented as open-source script coded in MATrix LABoratory (MATLAB).

2.4. Verification of developed numerical models

We used a simple case to test FE and FD simulation performances. We employed a rectangular aquifer as a synthetic case study introduced by Illangasekare and Döll (1989) and then compared the aquifer's analytical and simulated values (see Figure 2). This synthetic aquifer has two no-flow boundaries on the left and right sides and two constant boundaries with a value of 100 m in the top and bottom portions. The hydrodynamic parameters such as specific yield and transmissivity were also considered 0.15 and 885.71 m2/day,

respectively. Groundwater table drawdown was simulated for 210 consecutive days. The temporal variability of the groundwater level was daily recorded at the 85th node.

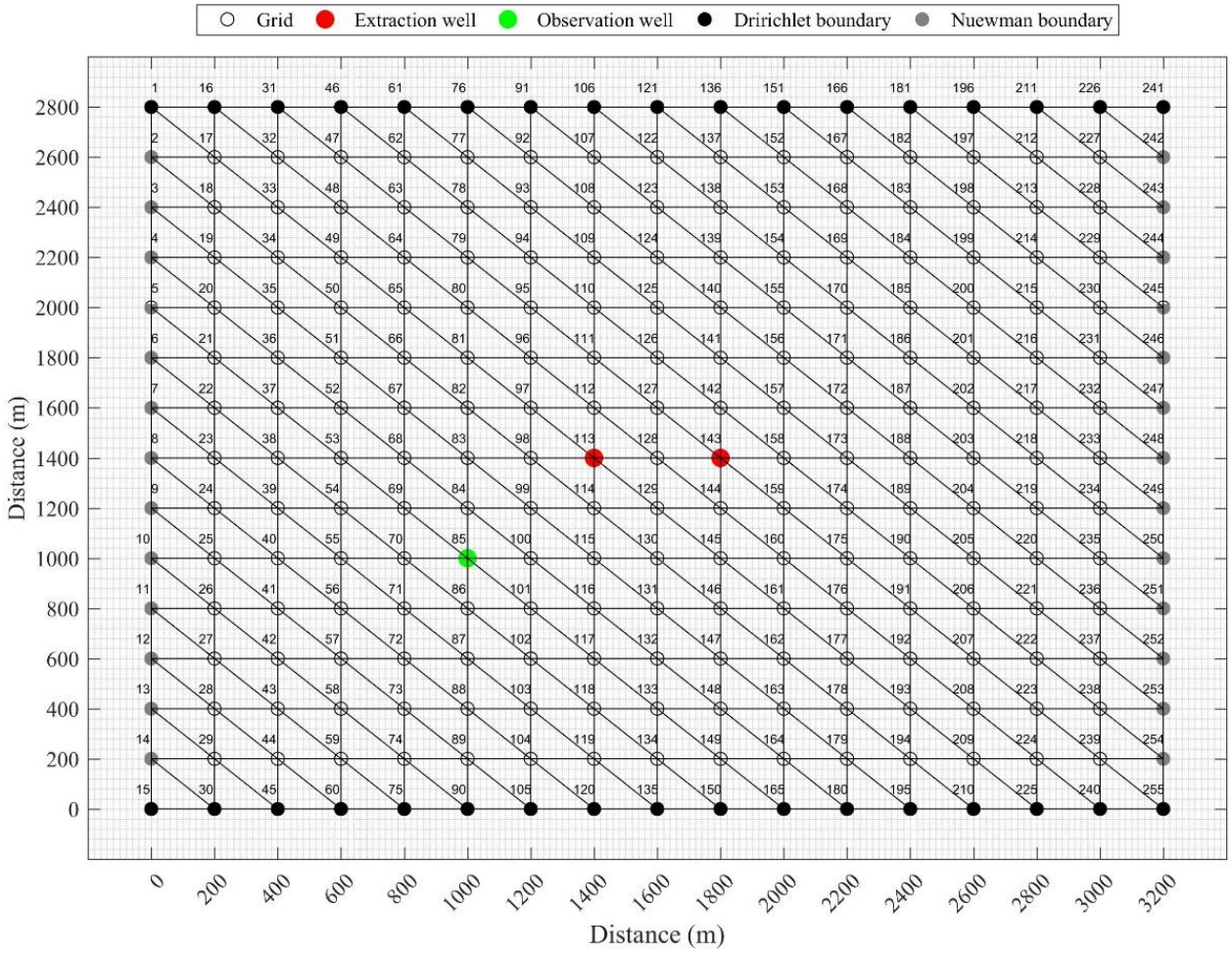

Fig. 2. Schematic representation of the elimination of the synthetic aquifer and identification of key structural features. The red solid circles denote the locations of extraction wells, and the green node indicates the location of the observation well. The distribution of the element matrix is displayed using gray triangles, illustrating the spatial discretization of the aquifer model. This visualization highlights the essential features of the aquifer and facilitates the interpretation of simulation results.

Simultaneously with the implementation of the FE and FD models, in order to simulate the groundwater level in the synthetic aquifer, it is necessary to calculate the analytical drawdown to evaluate the quality degree of the open-sources-based numerical methods. In this study, the analytical solution was calculated using image wells and the Tice equation. Figure (3) illustrates the image well structure along with actual wells.

The analytical drawdown of groundwater level is given by:

$$S_a = \left[\begin{array}{l} \frac{Q_1}{4\pi t}\left(W(u_1)+W(u_{IW1})-W(u_{IW3})\right)+ \\ \frac{Q_2}{4\pi t}\left(W(u_2)+W(u_{IW2})-W(u_{IW4})\right) \end{array} \right] \quad (8)$$

where,

$$u = \frac{r^2 S_y}{4Tt}$$

where the value of well function ($W(u)$) is determined through hydrodynamic argument (u). Also, Q1, Q2 indicate the discharge rate of extraction well ($m^3.day^{-1}$), while t and r denote, respectively, time (day) and the Euclidean distance (m). As shown, any actual extraction well has one image extraction well (IW_1 or IW_2) and one injection well (IW_3 or IW_4), and the image and actual wells' radius

from observation wells (85th node) was displayed via gray solid line. Further, the well function of actual and image wells was calculated considering different *u*-hydrodynamic factor. The extraction image wells were inserted in the left side of Neuman boundary and injection image wells were located in the bottom of constant boundary.

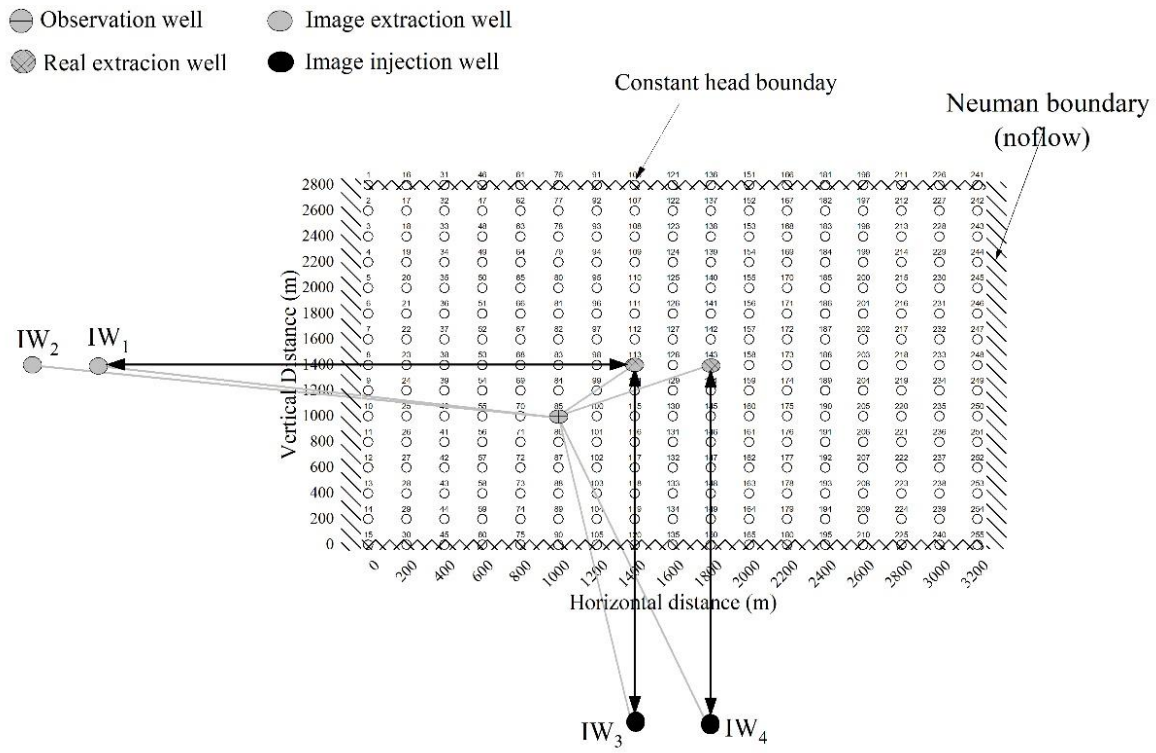

Fig. 3. The schematic representation of image and actual wells in the synthetic aquifer. It shows the location of extraction image wells represented by a grey circle and injection image wells represented by a solid black circle. Additionally, the actual extraction wells were placed in the 113 and 143rd nodes, while the groundwater levels were recorded at the 85th node, which is marked by a red square.

Finally, RMSE and NSE indices were used to compare the analytical and simulated drawdown.

$$RMSE = \sqrt{\frac{\sum_{i}^{n}(S_p^i - S_a^i)^2}{n}} \quad (9)$$

$$NSE = 1 - \frac{\sum_{i}^{n}(S_p^i - S_a^i)^2}{\sum_{i}^{n}(S_a^i - \bar{S}_a)} \quad (10)$$

where RMSE and NSE are performance criteria, and S_a and S_p denote the analytical and simulated drawdown (m), while simulation period is indicated by n (day). Also $\bar{S}_a$ shows the average of analytical drawdown (m).

2.5. Simulation of Artificial Recharge

A defining scenario of artificial recharge to the synthetic aquifer is explained here. In this case, the groundwater rising due to an injection well, implanted at the position (1800 and 2200), with a rate of 1314 cubic meters per day (150 liters per second) during 1500 days. Also, the temporal variations of groundwater level were recorded at the position (1000 and 1800), and the rest of the conditions and hydrodynamic components of the aquifer were assumed to be similar to the pumping test mode (Section 2-5). Figure (4) illustrates the schematic view of this plan.

2.6. Heterogeneity and Anisotropy Conditions

For more examination, another testing scenario was designed, and its description was presented here. In order to analyze the effect of regional variability of hydrodynamic coefficients on groundwater rising, a new geology structure was implemented. In this case, two different geological structures with different hydrodynamic features were defined. Since the injection well location and its

conditions are among the challenges in artificial recharge, its effects are addressed here (Figure 5). In this scenario, the transmissivity and specific yield of the injection zone were considered different. As such, the transmissivity and specific yield in the zone including the observation well were assumed to be 885.71 square meters per day and 0.1, respectively. While this factor for the injection zone was considered at 1328.565 and 442.855 square meters per day.

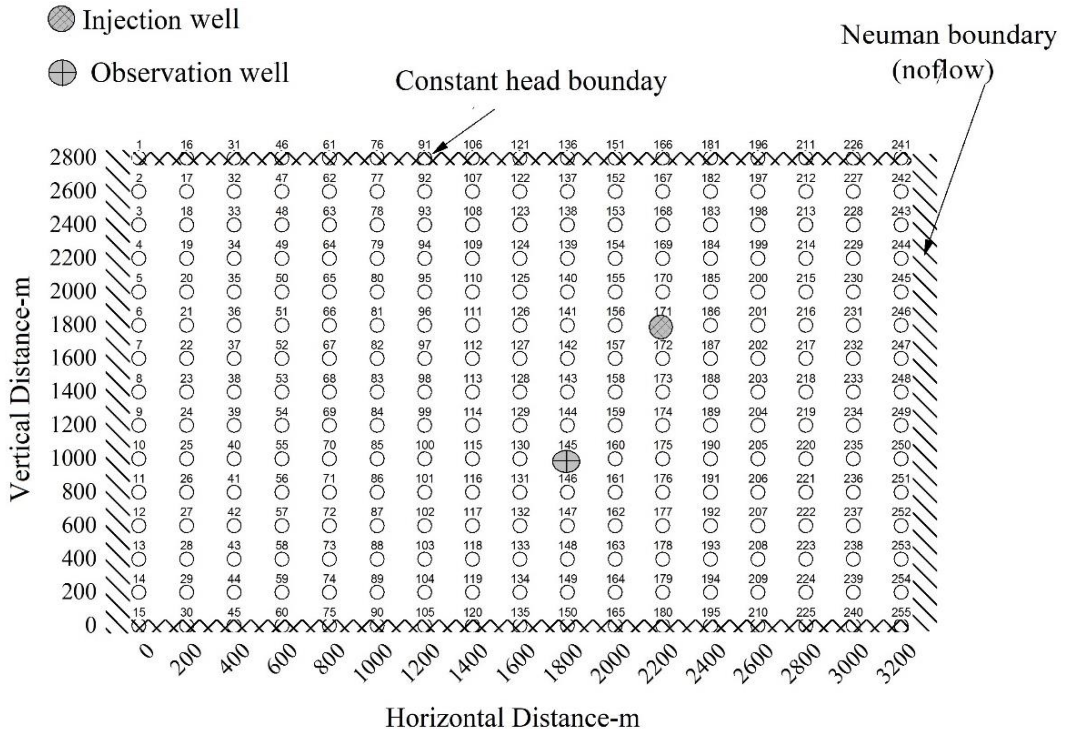

Fig. 4. A Representing view to define the synthetic aquifer for artificial recharge

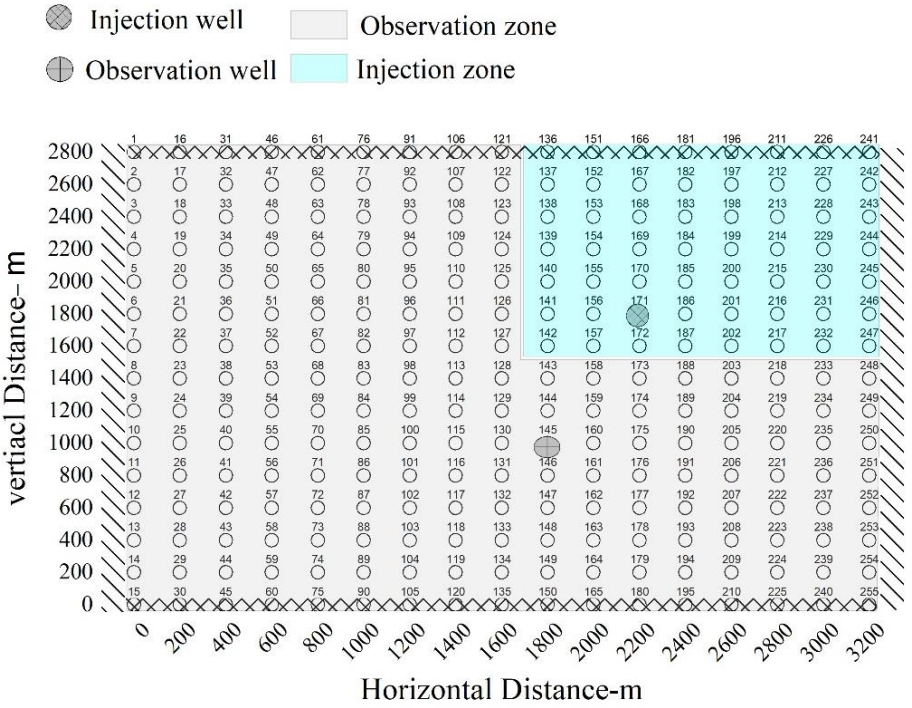

Fig. 5. A visual illustration defining heterogeneity and anisotropy conditions

Also, the specific yield for this zone was assumed as 0.09 and 0.3. The definition of this scenario was shown in Figure (5).

3. Results and Discussion

3.1.Performance Evaluation of Numerical Methods

First, the results related to the performance evaluation of numerical methods are presented in terms of RMSE and NSE criteria (Table 1). According to obtained results listed in this table, it can be said that both methods have good agreement with analytical solutions. However, a more detailed evaluation confirms that the accuracy of the FE method is better than the FD outputs.

Table 1. The performance results of two numerical methods

Method	RMSE (cm)	NSE
FE	0.615	0.98
FD	0.977	0.94

Figure (6) also shows the cumulative groundwater level drawdown simulated compared to the analytical solution. Like the results deduced from the evaluation indices, this figure approves that the FE model works better than the FD model. Another point that is a significant increase in error has been taking place on both methods during the final days of the experiment. So both finite difference and finite element methods are associated with an underestimation at the end of the experiment. The value of analytical drawdown was calculated 42.5 cm in the end of the experiment. While this value for FE and FD model was obtained 39.2 and 38.1respectively. This result has a good agreement with the derived findings of Simpson and Clement (2003) and Akbarpour et al. (2020) who stated that FE efficiency is stronger for groundwater modeling than FD.

Further, Figure (7) shows the spatial distribution of the groundwater level derived through both methods. As can be seen, in the area near the upper and lower borders of the aquifer the lowest drawdown took place, while at the location of the two pumping wells, the groundwater level dropped the most. It is worth noting the importance of acknowledging structural uncertainty in numerical modeling. As demonstrated in the preceding section, the groundwater level simulation in an aquifer was performed using two different numerical models. Despite using the same conceptual model, the results obtained from the two methods differed significantly. This highlights the significance of structural uncertainty in numerical modeling, which is often overlooked in such studies. Therefore, it is essential to consider and address this type of uncertainty in order to obtain more accurate and reliable results.

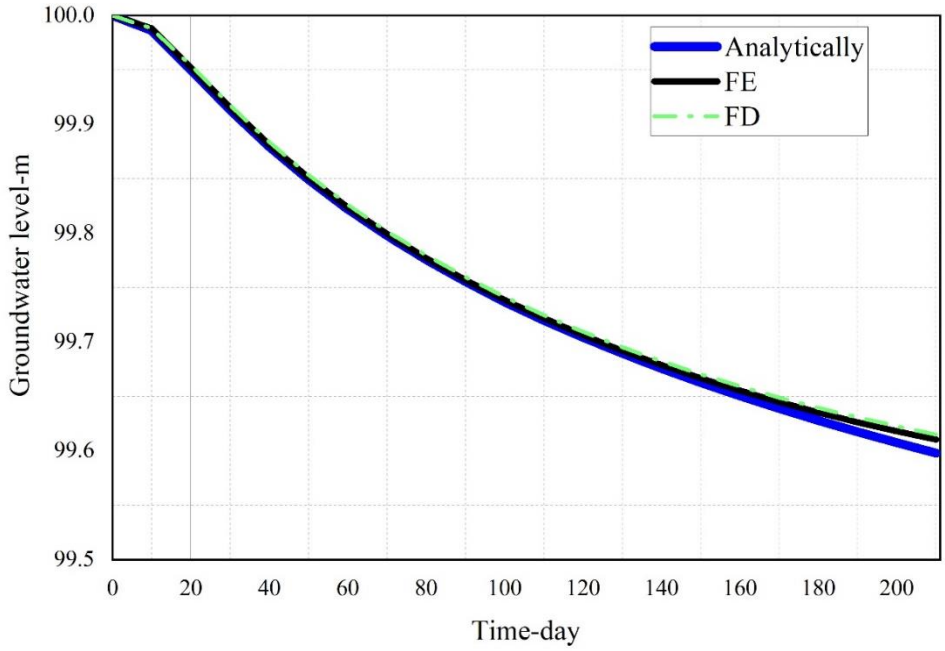

Fig. 6. Comparison analytical solutions vs groundwater simulated by FE and FD

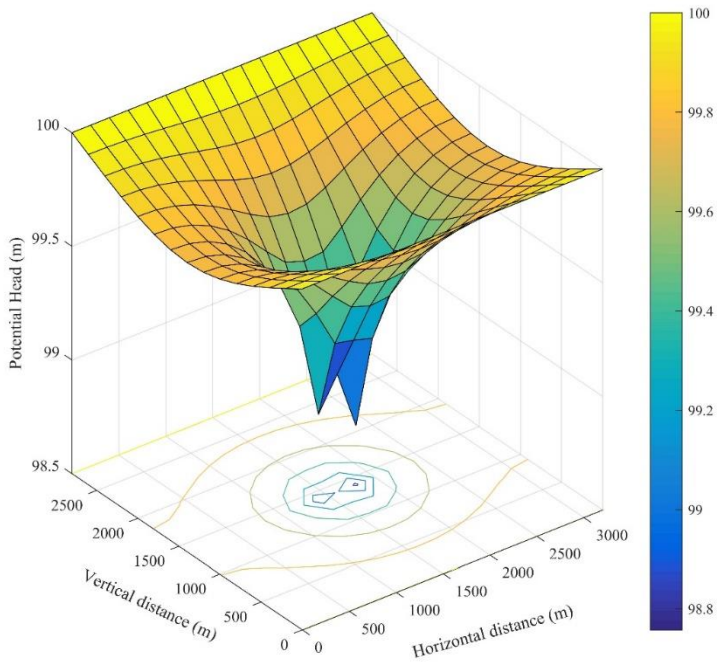

Fig. 7. A spatial variability of groundwater level due to extraction wells

3.2.Simulation of Artificial Recharge

This section presents results related to the simulation of the groundwater rising caused by the artificial recharge (scenario 1, see Figure 8). Based on the numerical results, the amount of groundwater level rise in the two methods of FE and the FD was obtained, respectively, a maximum of 90 cm. The results show a slight difference between the two numerical methods in the rise of the underground water level. Also, the rise in the FE method is associated with a greater slope than the FD. At this point, the rising rate of both has become practically stable. To better compare the performance of two numerical methods in simulating the effects of injection wells and groundwater level rise, the distribution of groundwater level rise is shown in Figure (8). Comparison of upwelling at boundaries and injection wells.

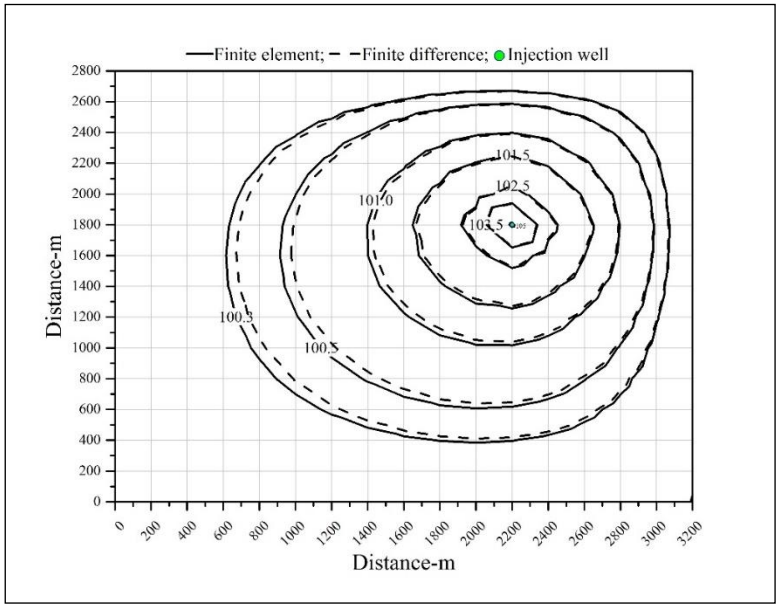

Fig. 8. Spatial distribution of groundwater level resulting from injection recharge.

3.3. Parameter Sensitivity Analysis of Artificial Recharge

By changing the values of transmissivity and specific yield components and keeping other components of the aquifer constant, the sensitivity analysis of each of the above-mentioned two components was investigated. For this purpose, the transmissivity value was changed from +25% to -25% in relation to 885.71 square meters per day. To better examine specific yield impact, it was assumed the same tolerance for both scenarios. The purpose was to compare the effect of a similar tolerance for the increase and reduction of specific yield. Also, three different values of 0.09, 0.1, and 0.3 were considered to investigate the effect of specific yield on the groundwater level rise.

The effect of transmissivity variability was formulated in two numerical methods, and the rising groundwater level was drawn in Figure (9). As shown, the decrease in transmissivity has increased the rate of groundwater level rise. The comparison of the amount of water rise at the end of the recharge confirms that in both FE and FD methods, a 25% reduction in transmissivity has led to a 100% increase in the groundwater level. Also, the 25% increase in transmissivity generated a 20% decrease in the amount of groundwater rising. Also, the results of this comparison reveal that as transmissivity increases, the difference between the two numerical methods propagates.

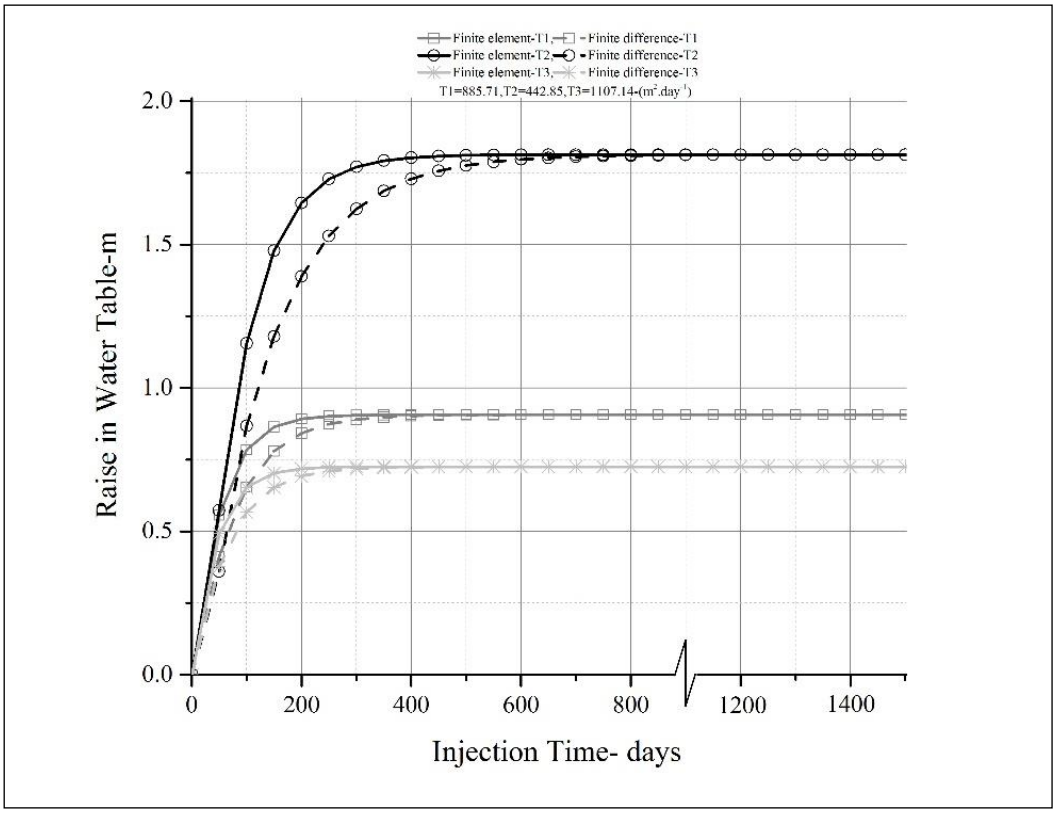

Fig. 10. The effect of specific yield on groundwater rising

In proceed, an attempt has been made to compare the impact of specific yield on groundwater rise using two methods, as illustrated in Figure 10. The results indicated that as the specific yield increases, the time required to reach a stable phase reduces, and the estimates obtained from the two methods (FE and FD) become more similar. In all three specific yield values tested, the FD method predicted lower values than the FE method. These findings provide insights into the importance of accurate estimation of specific yield in groundwater modeling and management. The implications of these results are discussed in detail in the subsequent sections of the paper.

Overall, the findings indicate that the impact of transmissivity on groundwater rise is more significant than that of specific yield, as illustrated in Figures 9 and 10.

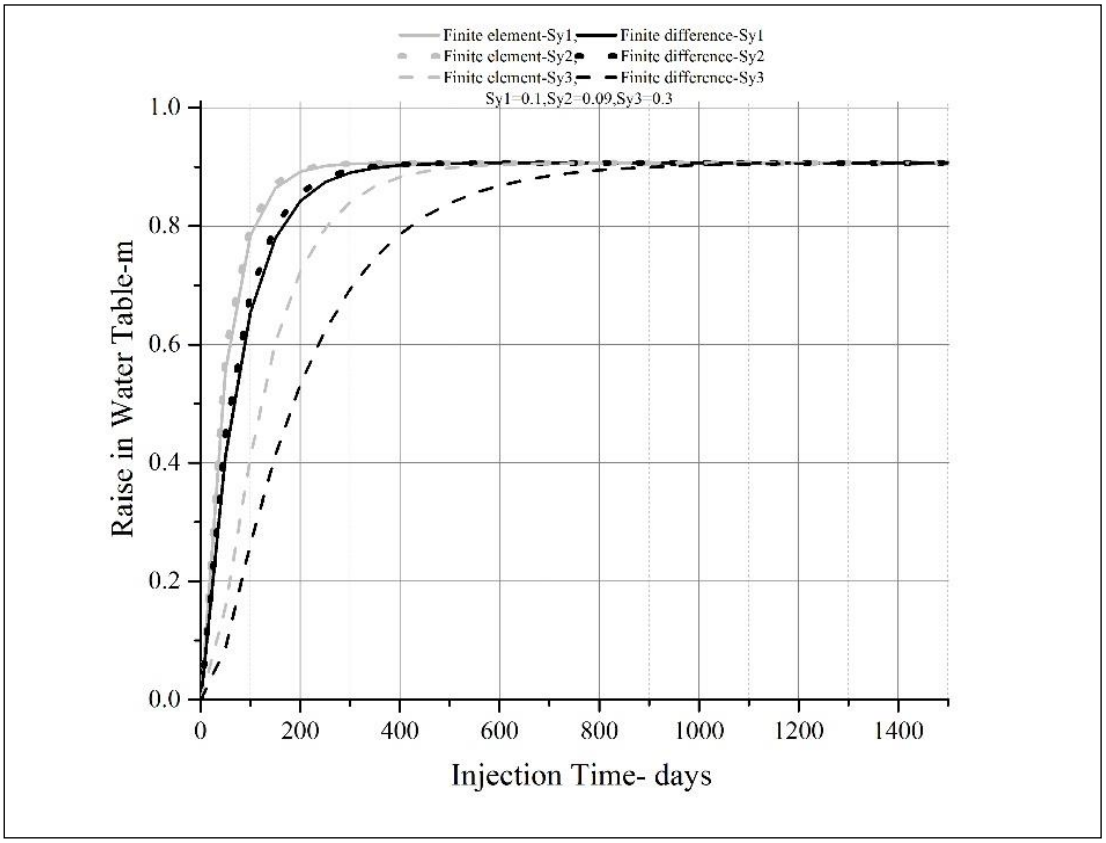

Fig. 10. The effect of specific yield on groundwater rising

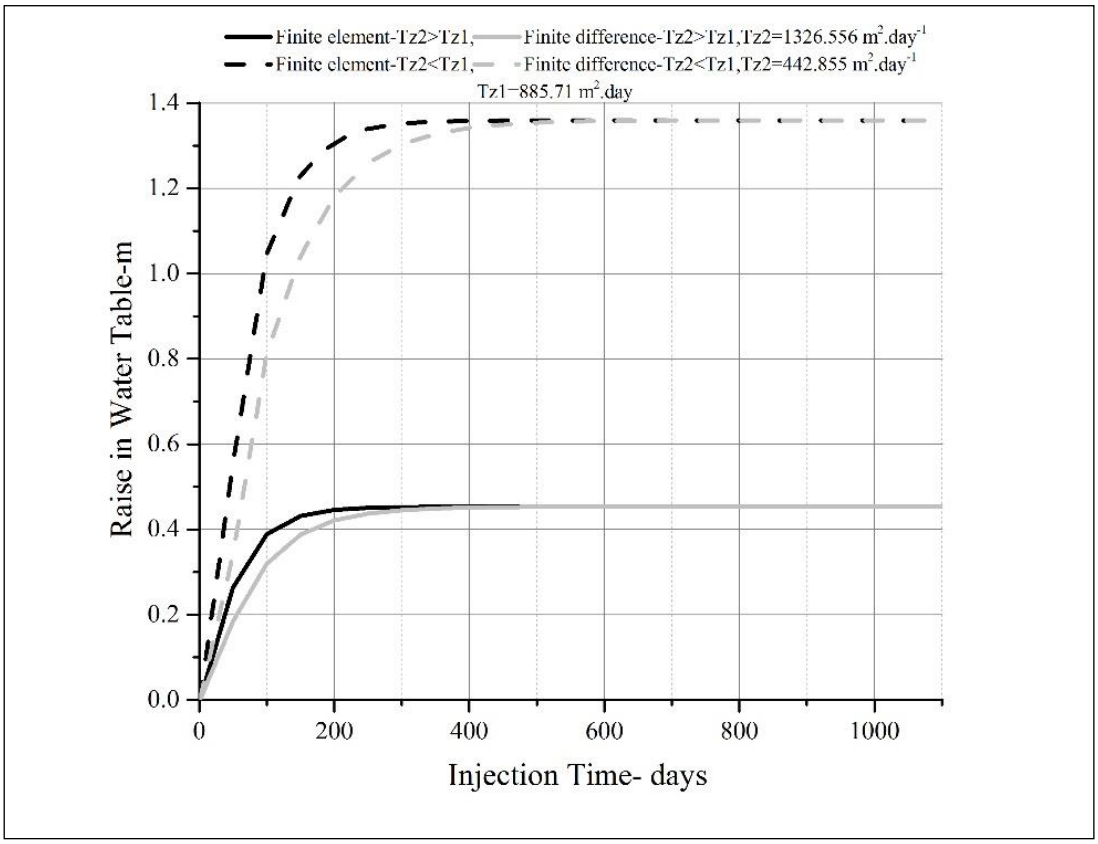

Fig. 11. Illustrating the effect of zonal variability of transmissivity on groundwater rising

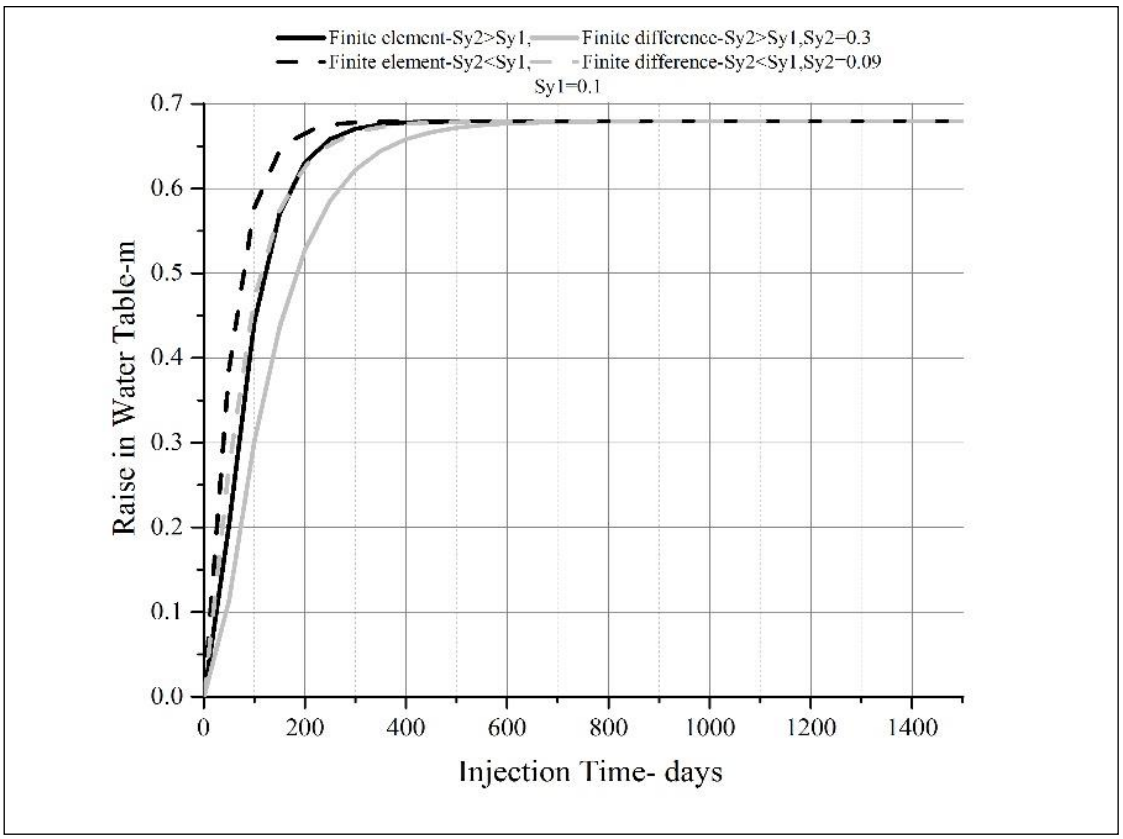

Fig. 12. Illustrating the effect of specific yield on groundwater rising

The analysis of regional variability further supports this conclusion, showing that lower transmissivity in the injection zone results in greater groundwater rise (Figure 9). Additionally, Figure 11 demonstrates that specific yield tolerance in the injection well area has a relatively minor effect on groundwater level rise compared to transmissivity.

These results provide valuable insights into the complex interplay between hydrogeological factors and groundwater recharge, demonstrating the importance of considering both transmissivity and specific yield in managing groundwater resources. Based on the findings, it can be concluded that the implementation of an injection well in a location with lower specific yield and transmissivity will result in a rapid rise in the groundwater level.

This observation can be attributed to the geological properties of the aquifer, where regions with lower specific yield have limited pore space and thus retain more water upon recharge. The ability of the developed numerical model to accurately simulate this phenomenon underscores its effectiveness in modeling groundwater recharge processes.

4. Conclusion

It is necessary to create a new plan regarding the management policies of these resources, due to critical conditions for groundwater resources. Hence, aquifer regeneration through artificial recharge is one of the most important basic solutions in this category. Locating injection well and considering the effect of aquifer features are the most important issues that have always been a challenge for researchers.

This study addressed the ability of two developed numerical methods as open-source coded in MATLAB environment to simulate the effect of an artificial recharge through injection well in a synthetic aquifer. For this purpose, three scenarios were defined to evaluate the performance of numerical methods (comparison of analytical and numerical solutions), simulating the rise of the groundwater level, and analyzing the sensitivity of the hydrodynamic features of the aquifer.

The performance evaluation results confirmed that the accuracy of the FE method in estimating the drawdown due to extraction is better than the FD. The experiment's results of artificial recharge into the aquifer through the injection well also showed that the groundwater level rise in the FE method is faster than in the

finite difference method. Also, after 1500 days of recharge, the height of the groundwater level is up to about 90 cm.

The results approved that the lower transmissivity in the injection zone compared makes further groundwater rising. Also, it was inferred that imposing an injection well in a zone with lower specific yield and transmissivity will more rise groundwater level.

5. Disclosure statement

No potential conflict of interest was reported by the authors.

6. References

Akbarpour, A., Zeynali, M. J., & Nazeri Tahroudi, M. (2020). Locating optimal position of pumping Wells in aquifer using meta-heuristic algorithms and finite element method. *Water Resources Management*, *34*, 21-34.

Arnold, J. G., Allen, P. M., & Bernhardt, G. (1993). A comprehensive surface-groundwater flow model. *Journal of hydrology*, *142*(1-4), 47-69.

Fletcher, S., Strzepek, K., Alsaati, A., & de Weck, O. (2019). Learning and flexibility for water supply infrastructure planning under groundwater resource uncertainty. *Environmental Research Letters*, *14*(11), 114022.

Hamidian, A. H., Razeghi, N., Zhang, Y., & Yang, M. (2019). Spatial distribution of arsenic in groundwater of Iran, a review. *Journal of Geochemical Exploration*, *201*, 88-98.

Hamraz, B., Akbarpour, A., Pourreza Bilondi, M., & Sadeghi Tabas, S. (2015). On the assessment of ground water parameter uncertainty over an arid aquifer. *Arabian journal of Geosciences*, *8*, 10759-10773.

Hora, T., Srinivasan, V., & Basu, N. B. (2019). The groundwater recovery paradox in South India. *Geophysical Research Letters*, *46*(16), 9602-9611.

Hussain, M. I., Muscolo, A., Farooq, M., & Ahmad, W. (2019). Sustainable use and management of non-conventional water resources for rehabilitation of marginal lands in arid and semiarid environments. *Agricultural water management*, *221*, 462-476.

Illangasekare, T. H., & Döll, P. (1989). A discrete kernel method of characteristics model of solute transport in water table aquifers. *Water Resources Research*, *25*(5), 857-867.

Jafarzadeh, A., Khashei-Siuki, A., & Pourreza-Bilondi, M. (2022). Performance assessment of model averaging techniques to reduce structural uncertainty of groundwater modeling. *Water Resources Management*, *36*(1), 353-377.

Jafarzadeh, A., Pourreza-Bilondi, M., Akbarpour, A., Khashei-Siuki, A., & Samadi, S. (2021). Application of multi-model ensemble averaging techniques for groundwater simulation: synthetic and real-world case studies. *Journal of Hydroinformatics*, *23*(6), 1271-1289.

Javandel, I., & Witherspoon, P. A. (1968). Application of the finite element method to transient flow in porous media. *Society of Petroleum Engineers Journal*, *8*(03), 241-252.

Liu, J., Shahroudy, A., Perez, M., Wang, G., Duan, L. Y., & Kot, A. C. (2019). Ntu rgb+ d 120: A large-scale benchmark for 3d human activity understanding. *IEEE transactions on pattern analysis and machine intelligence*, *42*(10), 2684-2701.

Mackay, J. D., Jackson, C. R., & Wang, L. (2014). A lumped conceptual model to simulate groundwater level time-series. *Environmental Modelling & Software*, *61*, 229-245.

Maquin, M., Mouche, E., Mügler, C., Pierret, M. C., & Viville, D. (2017). A soil column model for predicting the interaction between water table and evapotranspiration. *Water Resources Research*, *53*(7), 5877-5898.

McDonald, M. G., & Harbaugh, A. W. (1988). *A modular three-dimensional finite-difference ground-water flow model*. US Geological Survey.

Mohammadi, A. A., Zarei, A., Esmaeilzadeh, M., Taghavi, M., Yousefi, M., Yousefi, Z., ... & Javan, S. (2020). Assessment of heavy metal pollution and human health risks assessment in soils around an industrial zone in Neyshabur, Iran. *Biological trace element research*, *195*, 343-352.

Norouzi, H., & Shahmohammadi-Kalalagh, S. (2019). Locating groundwater artificial recharge sites using random forest: a case study of Shabestar region, Iran. *Environmental Earth Sciences*, *78*, 1-11.

Pacheco, F. A. L., Martins, L. M. O., Quininha, M., Oliveira, A. S., & Fernandes, L. S. (2018). Modification to the DRASTIC framework to assess groundwater contaminant risk in rural mountainous catchments. *Journal of Hydrology*, *566*, 175-191.

Sadeghi, A. R., & Hosseini, S. M. (2023). Assessment and delineation of potential groundwater recharge zones in areas prone to saltwater intrusion hazard: a case from Central Iran. *Environmental Monitoring and Assessment*, *195*(1), 203.

Sardo, M. S., & Jalalkamali, N. (2022). A system dynamic approach for reservoir impact assessment on groundwater aquifer considering climate change scenario. *Groundwater for Sustainable Development*, *17*, 100754.

Shepley, M. G., & Soley, R. W. N. (2012). The use of groundwater levels and numerical models for the management of a layered, moderate-diffusivity aquifer. *Geological Society, London, Special Publications*, *364*(1), 303-318.

Simpson, M. J., & Clement, T. P. (2003). Comparison of finite difference and finite element solutions to the variably saturated flow equation. *Journal of hydrology*, *270*(1-2), 49-64.

Xu, T., Valocchi, A. J., Ye, M., Liang, F., & Lin, Y. F. (2017). Bayesian calibration of groundwater models

with input data uncertainty. *Water Resources Research*, *53*(4), 3224-3245.

Zaresefat, M., Ahrari, M., Reza Shoaei, G., Etemadifar, M., Aghamolaie, I., & Derakhshani, R. (2022). Identification of suitable site-specific recharge areas using fuzzy analytic hierarchy process (FAHP) technique: a case study of Iranshahr Basin (Iran). *Air, Soil and Water Research*, *15*, 11786221211063849.

Zienkiewicz, O., Mayer, P., & Cheung, Y. K. (1966). Solution of anisotropic seepage by finite elements. *Journal of the Engineering Mechanics Division*, *92*(1), 111-120.